Atmósfera 39, 673-697 (2025)
https://doi.org/10.20937/ATM.53476

Intensities of the 2023 and 2024 heatwaves in different local climate zones of the city of Puebla (Mexico)

Adalberto TEJEDA-MARTÍNEZ[1]*, Irving Rafael MÉNDEZ-PÉREZ[2], Juan Pablo BÁEZ-VÁSQUEZ[3], Elda LUYANDO-LÓPEZ[4], Gabriel BALDERAS-ROMERO[3], Cecilia CONDE-ÁLVAREZ[4] and Aranza E. BARUCH-VERA[5]

[1] *Grupo de Climatología Aplicada de la Universidad Veracruzana, 91090 Xalapa, Veracruz, México.*
[2] *Centro de Ciencias de la Tierra de la Universidad Veracruzana, 91090 Xalapa, Veracruz, México.*
[3] *Departamento de Investigaciones Arquitectónicas y Urbanísticas, Benemérita Universidad Autónoma de Puebla, Puebla, 72000 Puebla, Puebla, México.*
[4] *Instituto de Ciencias de la Atmósfera y Cambio Climático, Universidad Nacional Autónoma de México, 04510 Ciudad de México, México.*
[5] *Maestría en Ciencias de la Tierra de la Universidad Veracruzana, 91090 Xalapa, Veracruz, México.*
*Corresponding author; email: atejeda.martinez@gmail.com

Received: March 5, 2025; Accepted: September 25, 2025

RESUMEN

Durante 2023 y 2024, México experimentó olas de calor intensas que afectaron amplias zonas del país. En este artículo se evalúa la respuesta diferenciada de tres olas ocurridas en 2023 y cuatro en 2024 en cinco zonas climáticas locales (LCZ, por su sigla en inglés) de la ciudad de Puebla (México), siguiendo el criterio de cinco días consecutivos en que las temperaturas diarias rebasaron el percentil 90, aplicado a las temperaturas máximas (27.4 ºC) para las olas diurnas y a las mínimas (17.4 ºC) para las olas nocturnas. Las olas se clasificaron como circadianas cuando fueron diurnas y nocturnas en las mismas fechas. La intensidad de las olas se calculó en días-grado y en horas-grado para obtener mayor precisión. Adicionalmente, se aplicó el índice Humidex para estimar los efectos bioclimáticos en horas-grado por encima del valor del Humidex preferente. Se encontró que las olas nocturnas en el centro de la ciudad son más intensas, probablemente debido a la isla de calor urbana, y que las LCZ con mayor vegetación incrementan la intensidad de las olas si se incorpora a su evaluación la contribución de la humedad atmosférica. Se utilizaron datos termohigrométricos tomados cada 15 min en cinco estaciones meteorológicas durante 2023 y durante seis meses de 2024. Como en México no abundan los trabajos que evalúen los efectos diferenciados en distintas zonas de una ciudad, se seguirá este enfoque en el presente artículo.

ABSTRACT

In 2023 and 2024, Mexico experienced intense heatwaves that affected large areas of the country. This article evaluates the differentiated responses of three events in 2023 and four in 2024 in five local climate zones (LCZ) in the city of Puebla (Mexico). Heatwaves were identified based on the criterion of five consecutive days in which daily temperatures exceeded the 90th percentile, applied to the maximum temperature (27.4 ºC) for diurnal waves and to the minimum temperatures (17.4 ºC) for nocturnal waves. When thermal thresholds were exceeded during both day and night over the same period, waves were classified as circadian. To achieve greater precision, the wave's intensity was calculated in degree-days and degree-hours. Additionally, the Humidex index was applied to estimate the bioclimatic effects in degree-hours above the preferred Humidex value. The findings indicate that nocturnal waves in the city center are more intense, partly due to the urban heat island effect, and that LCZ with greater vegetation show increased wave intensity when

atmospheric humidity is included in the analysis. Thermohygrometric data recorded every 15 min at five meteorological stations throughout 2023, and six months of 2024, were used. Given the limited number of studies in Mexico evaluating the spatially differentiated effects of heatwaves within urban areas, this study adopts a localized approach.

Keywords: degree-hours, heatwaves, human bioclimate, Humidex, local climate zones.

1. Introduction

So far this century, the frequency and intensity of heatwaves have increased, producing adverse effects on health, ecosystems, agriculture, and the economy (Campbell et al., 2018; IPCC, 2023; Wang et al., 2023). One of the most extreme examples is the European 2003 heatwave, which resulted in the loss of between 50 000 and 70 000 human lives (de Bono et al., 2004; Robine et al., 2008). The criteria and methodologies for evaluating heatwaves are not unique, mainly because the diversity of climatic, social, and cultural conditions worldwide, which makes it difficult to apply a uniform approach (Perkins and Alexander, 2013). Moreover, the effects of heatwaves are not limited to those caused only by high temperatures; they are also accompanied by indirect effects attributable to other meteorological variables, such as atmospheric humidity (Cheng et al., 2024; Narayanan et al., 2025), solar radiation —whose evaluation indoors and shaded assessment remains complex— and wind, for which detailed information is often lacking. Regarding temperatures, not only daily maximums have an impact, but also nighttime temperatures, which can have notable consequences for vulnerable populations such as the elderly and infants (Gosling et al., 2009; Zhou et al., 2024).

There are several antecedents of studies of heatwaves in Mexico that reflect the growing concern about rising temperatures in urban environments. Jáuregui (2009) reported that the number of days exceeding the 30 ºC threshold in Mexico City between 1991 and 2000 was twice that of the previous two decades and nine times that of 1870. This increase was attributed to the effects of urbanization on ambient temperatures (Jáuregui, 1997, 2000). His findings highlight how urban growth has intensified both the frequency and intensity of heatwaves, providing a foundational reference for understanding long-term climatic trends in the region.

An extreme case, given its already very hot summers, is the city of Mexicali, located in the desert region of northwestern Mexico, bordering the American Southwest. García-Cueto et al. (2010) reported that heatwaves—according to the criterion of three or more consecutive days above the 44 ºC threshold—tripled in the first decade of the 21st century compared to the 1970s. Martínez-Austria et al. (2016) observed for the same city that, from the 1960s to 2010, the number of times in which the average July daily maximum temperature (42.3 ºC) was exceeded increased from less than 10 times to more than 20.

Studies have shown that the diverse landscape and topographic configurations within cities lead to spatial variability in heatwave behavior. This has been documented in Brno, Czech Republic (Geletič et al., 2018); in Guadalajara, Mexico, through satellite-based assessments of extreme heat risk (López-García, 2018); and in Mexico City, using a network of meteorological stations (Vargas and Magaña, 2020).

In the case of Puebla, research on the urban climate began over half a century ago. Gäb (1970, 1976) conducted the first studies on the urban heat island (UHI), reporting that the city center tended to be warmer than surrounding areas with higher elevation and vegetation cover, which were 2 to 4 ºC cooler. These findings provided early evidence of the relationship between land cover, elevation, and local temperature variation in the region.

Towards the end of the 20th century and the beginning of the 21st, the topic was revisited in several studies (Balderas-Romero et al., 2009; Balderas-Romero, 2018). Around 1997, thermohygrometric measurements were conducted using a vehicle equipped with sensors, during nocturnal transects from the periphery to the city center on clear nights (3:00 to 6:00 LT), under stable atmospheric conditions with calm or light winds. On both a cold season night (February 28) and a warm season night (May 11), a UHI was detected, with a contrast of 13 ºC

in the center of the city compared to 10 ºC in the rural periphery, on the former date, and from 17 to 14 ºC on the latter (Balderas-Romero, 2018). By April 2007, similar but contrasting patterns were observed. Balderas-Romero (2018) identified that the warmest zones are typically located over urbanized territory, with a tendency to settle over the city center and extend towards the northwest, an area with a high density of human settlements. Temperature differences ranged from 2 to 3 ºC at night and 5 to 6 ºC during the day. These findings confirm that land use plays a relevant role in the behavior of both the UHI and heatwaves, as demonstrated by several studies (Zou et al., 2021; Mohammad-Harmay, 2022; Salau et al., 2025).

Global daily mean temperatures remained at record-high levels for nearly half of 2023 and much of 2024 (Ripple et al., 2024). In the case of Mexico, during 2023 and 2024, large areas were affected by extreme heatwaves, with temperatures reaching unprecedented levels. Initially, 2023 was classified as the driest year since 1942 and the warmest since 1953 (CONAGUA, 2024a). The summer of 2023 in the Northern Hemisphere was unusual due to extreme heat. In Mexicali, in the state of Baja California, a temperature of 51.4 ºC was recorded (WMO, 2024). Health impacts doubled in Mexico compared to 2022. In one semester, there were 4306 cases of heat stroke, dehydration, and burns, with 421 recorded deaths (DGE, 2023; CENAPRECE, 2024).

In 2023, the increase in sea surface temperature in most ocean basins, especially in the North Atlantic, contributed to global record temperatures. Several studies indicate that the El Niño phenomenon was one of the main factors associated with this global thermal increase (Voosen 2024; Marengo et al., 2025; Zhou et al., 2025).

The year 2024 has been the warmest on record globally, with average temperatures 0.72 ºC above the 1991-2020 mean and 1.60 ºC above pre-industrial levels (1850-1900). On July 22, the average global temperature reached an unprecedented 17.16 ºC (C3S, 2025). In Mexico, this anomalous warming was reflected in extreme temperature events across various regions. On May 9, 2024, 10 cities recorded their highest-ever temperatures. In Puebla, for instance, the record was broken with a maximum temperature of 35.2 ºC (CONAGUA, 2024b), breaking a 77-year-old record, and the next day, 35.6 ºC was reached (SMN, 2024). These record-breaking values occurred during officially recognized heatwave periods. However, in Mexico, heatwaves are defined using national-level dates established by the National Meteorological Service (one day above the 95th percentile), which do not always correspond to regional or local thermal behavior. For example, the third official heatwave of 2023 in Mexico spanned from June 1 to June 22, yet the onset, intensity, and duration of heat events varied markedly across local climates and urban configurations.

In his review of current literature on heatwaves—focusing on the physical processes that generate them, methods of analysis, and their impact both on natural and human ecosystems—McGregor (2024) highlights the complexity of establishing a universal definition of a heatwave that incorporates both physical and social dimensions. Boni et al. (2023) highlight the need for a multidisciplinary definition when a biophysical and sociopolitical phenomenon occurs.

The present research adopts the heatwave definition established by the former Expert Team on Climate Change Detection and Indices (ETCCDI; Zhang et al., 2011), which defines a heatwave as occurring when daily temperatures exceed the 90th percentile for five consecutive days. Maximum daily temperatures were used to identify diurnal heatwaves, while minimum daily temperatures were used for nocturnal ones. Furthermore, heatwaves were classified as circadian when both diurnal and nocturnal thresholds were exceeded on the same dates. The heatwave intensity was calculated in degree-days using the index proposed by Chen and Li (2017) and applied to China (1961-2010), and by García-Martínez and Bollasina (2021) for the United States and Mexico (1950-2005). To achieve greater precision, the index was adapted to calculate intensity in degree-hours. Additionally, the Humidex human bioclimate index, which accounts for the combined effects of air temperature and atmospheric humidity (Cvijanovic et al., 2023), was applied to estimate heatwave intensities in degree-hours above the preferred Humidex value.

In this article, the differentiated response of three waves in 2023 and four in 2024 will be evaluated across five local climatic zones in the city of Puebla. To support this work, a broad review and correction of the thermohygrometric data, recorded every

15 min throughout 2023 and the first half of 2024, was performed.

The next section (number 2) describes the study area, including its climatology and thermal trends, the meteorological stations used for this study, and their corresponding local climatic zones. Section 3 describes the data, its completeness, and the method used to impute missing data. The methodology for assessing heatwave intensity, detailed in section 4, builds upon the approach proposed by Chen and Li (2017) by incorporating hourly ambient temperature and atmospheric humidity data, allowing a transition from a purely thermal assessment to a bioclimatic analysis. The results are presented and discussed in section 5 graphically and descriptively, and conclusions are drawn in section 6.

2. Study zone

The municipality of Puebla, which contains the city of the same name (the fifth most populous in Mexico), is located in the central-western part of the state of Puebla (Mexico), with an area of 544.65 km^2. The city of Puebla is located between the parallels 18º 50' and 19º 14' N, and the meridians 98º 18' and 98º 01' W (INEGI, 2010). The location of the municipality in the Mexican territory and in the state of Puebla is shown in Figure 1. The urban area of the city of Puebla occupies about one-third of the municipality (SPCGIR, 2018).

The municipality is in the central sector of a broad open valley, flanked to the west by the mountain range that includes the Popocatépetl (5419 masl) and Iztaccíhuatl (5220 masl) volcanoes and to the north by the Matlalcuéyetl volcano, also known as La Malinche, which rises to 4420 masl (INEGI, 2024). The altitudes within the municipality range from 1980 to 4400 m, reaching their highest point near the summit of the La Malinche volcano. At an average elevation of 2140 masl, the terrain is a plain with a slight northeast-southwest slope (Flores-González and Ladino-Álvarez, 2018).

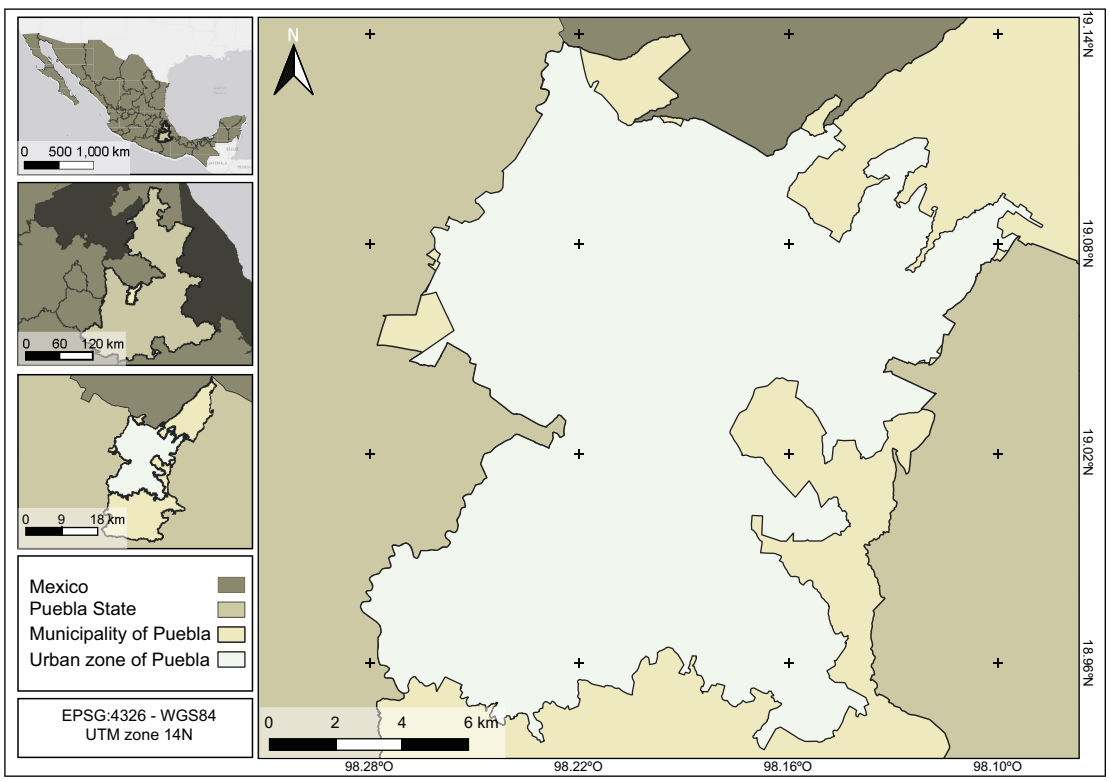

Fig. 1. Location of the municipality of Puebla. Own elaboration based on data from CONABIO (2024) and IMPLAN Puebla (2016).

2.1 Climatology

The municipality has two different climate areas. In most of its territory (96%), it has a temperate subhumid climate with rains in summer, and in the remaining area (4%), a semi-cold subhumid climate with rains in summer (INEGI, 2010).

The average annual temperature of the municipality ranges between 12 and 18 ºC, the maximum average annual temperature is in the range of 26 to 30 ºC in the southern region of the municipality, 22 to 26 ºC in the central metropolitan area, and 18 to 22 ºC in the northern part of the municipality. The ranges for annual average minimum temperatures are, for these respective regions, 12 to 18 ºC, 8 to 12 ºC, and 4 to 8 ºC. The average annual precipitation ranges between 400 and 800 mm (Vidal-Zepeda and Hernández-Cerda, 2007), depending on the specific area.

Winds are characterized by symmetrical behavior: northerly breezes at night and southerly winds during the day. A brief shift from the east typically occurs in the early afternoon, while calm conditions are most common during the night and morning until midday. The most intense ones occur between 12:00 and 18:00 LT, reaching speeds of between 4 and 8 m s^{-1}. The maximum average speed occurs in April and October (Balderas-Romero, 2018).

Since 2005, the Red Automática de Monitoreo Meteorológico (RAMM, Automatic Meteorological Monitoring Network) has been in operation, run by the Departamento de Investigaciones Arquitectónicas y Urbanísticas (DIAU, Department of Architectural and Urban Research) of the Benemérita Universidad Autónoma de Puebla, which consists of 20 Vantage II-type automatic wireless stations (Davis Instruments) installed on building rooftops, positioned at the upper limit of the urban canopy and the lower part of the atmospheric boundary layer. The five stations used in this work are shown in Figure 2, and their local climatic zones are detailed in Table I. These five meteorological stations were selected because they

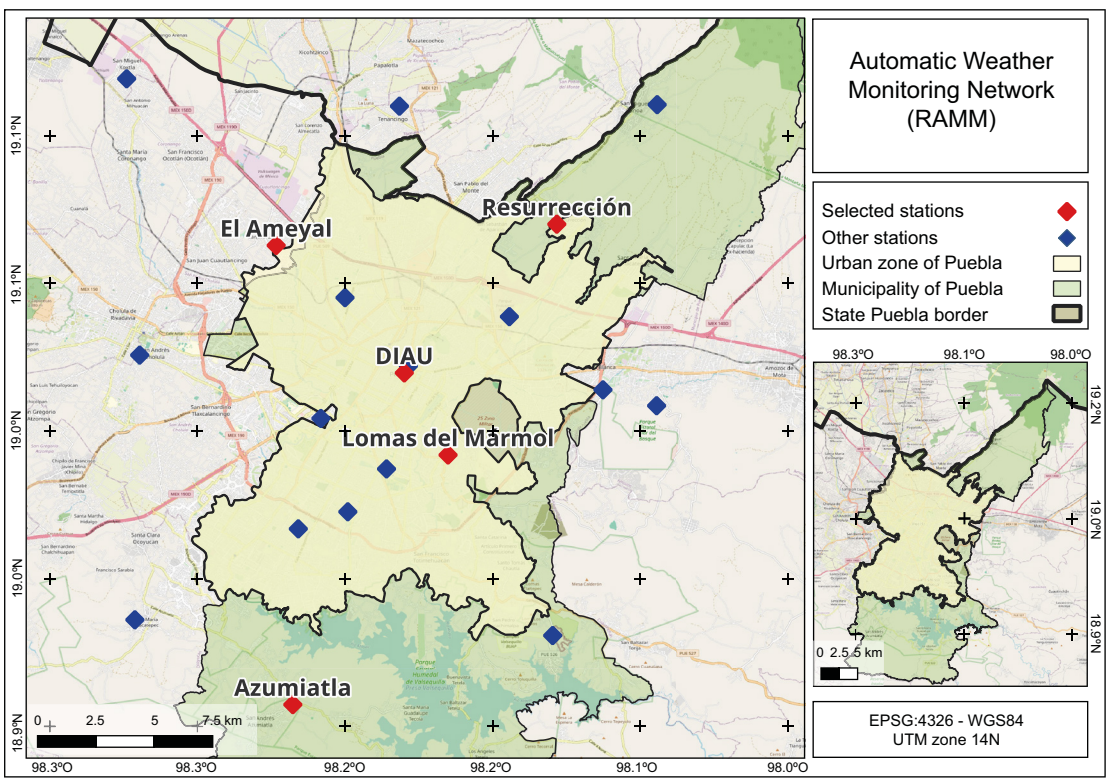

Fig. 2. Study area and location of the RAMM stations. Marked in red are those used in this work. Own elaboration based on data from CONABIO (2024) and IMPLAN Puebla (2016). (RAMM: Red Automática de Monitoreo Meteorológico [Automatic Meteorological Monitoring Network].)

Table I. Geographic location and local climatic zones (Stewart and Oke, 2012) of the five stations used in this work.

Name	Type		LCZ	Latitude (ºN)	Longitude (ºW)	Elevation (masl)
DIAU	Urban	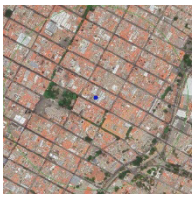	2_b: compact mid-rise buildings with scattered trees.	19º 02’ 38”	98º 11’ 47”	2153
Lomas del Mármol	Suburban		6: open low-rise buildings.	19º 00’ 38”	98º 10’ 43”	2131
Azumiatla	Rural		C_9: bushes with sparse buildings.	18º 54’ 33”	98º 14’ 30”	2125
El Ameyal	Suburban		D_6: low plants with open low-rise buildings	19º 05’ 58”	98º 15’ 47”	2160
Resurrección	Rural	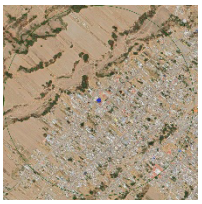	9: scattered buildings.	19º 6’ 15.41”	98º 8’ 3.95”	2340

LCZ: local climate zones.

had sufficient data to complete the information using the imputation method described in the data section.

Using RAMM temperature data, the thermal distribution of the Puebla valley was analyzed for 2007. In the lowest-elevation zones, average annual temperature ranged between 21 and 22 ºC, while values near the summit of La Malinche ranged between 4 and 5 ºC. To eliminate the altitude factor in the isotherm charts obtained from route measurements or from RAMM stations, a linear regression was applied, yielding a gradient vertical thermal temperature of –0.007 ºC m^{-1} (Balderas-Romero et al., 2009). The thermographic pattern obtained reflects, as expected, the modifying effects of urbanization (Balderas-Romero, 2018).

To detect the influence of the UHI superimposed on global climate change, Lemus-Flores (2016) quantified the number of days per each year in which the

ambient temperature of 30 ºC was exceeded at two locations: a suburban point 12 km southwest of the city center, influenced by a nearby body of water, and an urban point, characterized by commercial and residential buildings, 3.5 km south of the city center (see Table II). It is noteworthy that, as Lemus-Flores (2016) emphasizes, although the city center station is 56 m above the suburban station, it has recorded more days with temperatures above 30 ºC, which could in part be attributed to urban-induced atmospheric warming.

Table II. Number of days in which the temperature exceeded 30 ºC in a suburban point (Echeverría, 18º 58' 59" N, 90º 16'4 8" W, 2066 masl) and in the city center (18º 56' 24" N, 98º12' 0" W, 2122 masl). Adapted from Lemus-Flores (2016).

Decade	Suburban station	City center
1954-1963	52	180
1964-1973	70	156
1974-1983	52	265
1984-1993	35	143
1994-2003	18	200
2004-2013	27	328

To the current evidence of urban atmospheric warming, the trends of climate change indices were added (Zhang et al., 2011) in Table III for the DIAU urban station from 2008 to 2023 (shown in Fig. 3). The results are consistent: on one hand, the frequency of warm-related indices has doubled over those 16 years; on the other, the number of cool days has decreased by practically two-thirds. This warming is attributed to both global climate change and urbanization, and trends show it will continue. So, an increase in both the frequency and intensity of heatwaves is expected over time, with fluctuations induced by climate variability.

Table III. Climate change warm-related indices (Zhang et al., 2011) for the DIAU station from 2008 to 2023.

Description	Criterion
Summer days	$Tx > 25$ ºC
Cool days	$Tx <$ 10th percentile
Warm nights	$Tn >$ 90th percentile
Hot days	$Tx >$ 90th percentile

T_x: daily maximum temperature; T_n: daily minimum temperature.

Regarding atmospheric humidity, Gálvez-Vidal (2021) and Tejeda-Martínez et al. (2023) confirmed the inverse relationship between temperature and relative humidity, as Gäb (1976) had already shown. Gálvez-Vidal (2021) compared 10 recent years of daily vapor pressure between a site in the city center (DIAU station) and a suburban site (Lomas del Mármol), finding that the differences between them are minimal, almost insignificant. Tejeda-Martínez et al. (2023) reported that, in general terms, the city of Puebla presents a vapor content (absolute humidity) 3 to 5 g m^{-3} higher than in the rural environment during the diurnal period, with smaller differences at night that occasionally become inverse (–1 g m^{-3}) at dawn and dusk.

3. Data

For the period 2008-2023, the completeness of the data measured at 15-min intervals at the DIAU station was evaluated. The number of missing data is shown in Table IV.

Missing data were imputed based on the simple linear regression model:

$$y = 0.00824 + 1.03449x \quad (1)$$

where y is the temperature of the DIAU station and x that of the El Carolino station (19º 2' 34" N, 98º 11' 41" W, 2165 masl), which is located 200 m in a straight line from the DIAU station and at nearly the same elevation. The coefficient of determination of the imputation model is 96.7% and the standard error of estimate is 0.87 ºC with a significance level of 0.005. This imputation method was selected because linear regression models provide a systematic and effective approach for handling missing values in climate variables such as temperature, by accurately predicting missing data based on available observations (Kotsiantis et al., 2006). Furthermore, this technique has been among the most relevant methods for imputing missing values in climate data over the past decade (Alejo-Sánchez et al., 2025).

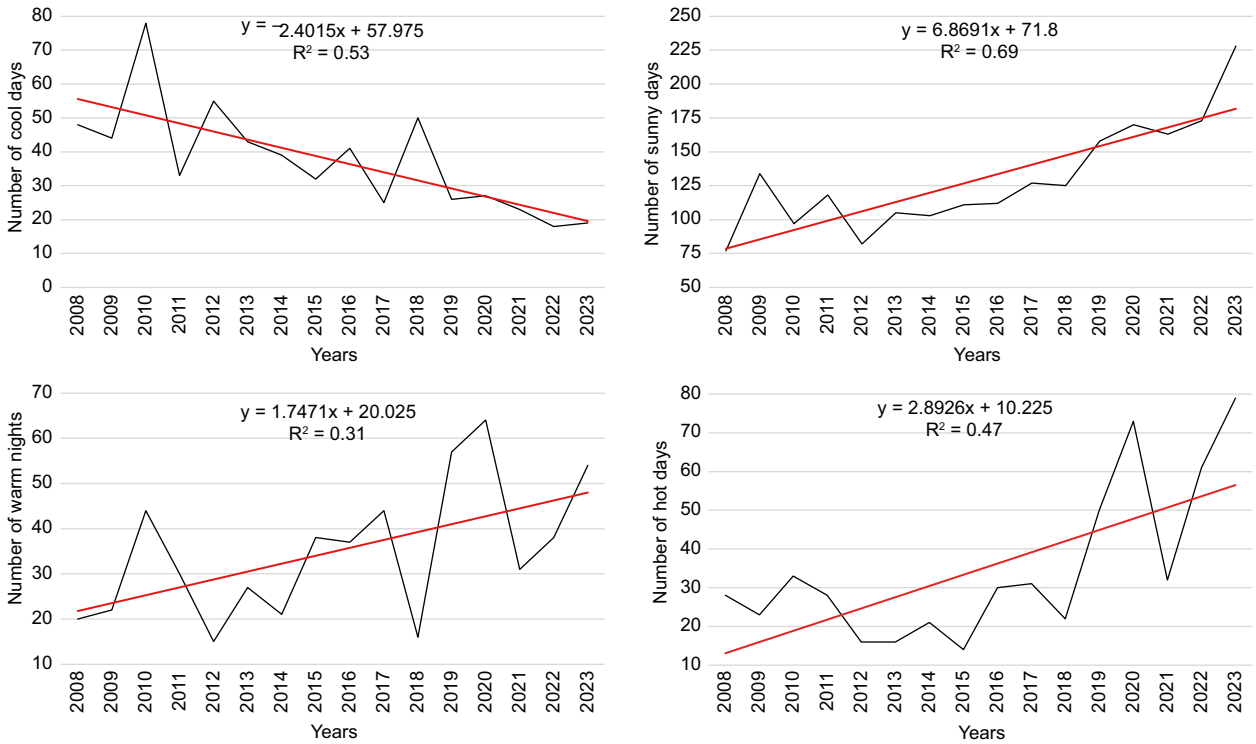

Fig. 3. Climate change indices for the DIAU station from 2008 to 2023: cool days, summer days, warm nights and hot days. Source: own elaboration.

Table IV. Number of missing data per year (2008-2023) from the DIAU station (total of 35 040 records per year).

Year	Missing data (%)	Year	Missing data (%)
2008	0.02	2018	0.14
2009-2013	0	2019	0.17
2014	0.17	2020	0.08
2015	0.01	2021	1.10
2016	0.03	2022	0
2017	0.09	2023	0

In the four non-urban stations used for this study, missing data were identified in the original 15-min interval records collected over the 18 months analyzed (12 in 2023 and six in 2024, that is, a total of 52 512 data). The proportion of missing data was 5% at El Ameyal, 4% at Lomas del Mármol, and 1% at Azumiatla and Resurrección. To complete the dataset, linear regression models were applied using observed data from paired stations, as shown in Table V for temperature and in Table VI for relative humidity.

4. Methodology

Heatwaves were identified based on the ETCCDI (Zhang et al., 2011) definition, that is, five consecutive days in which daily temperatures exceeded the 90th percentile of the 2008-2023 temperature series of the DIAU station, applied to maximum temperatures (90th percentile equal to 27.4 ºC) for diurnal waves and to minimum temperatures (90th percentile equal to 17.4 ºC) for nocturnal waves. When heatwaves are both diurnal and nocturnal on the same dates, they are considered circadian.

Thus, based on the threshold temperatures shown above and the criterion of five consecutive days, the dates of the heatwaves that occurred during 2023 and 2024 were identified, choosing those with the longest duration, regardless of the meteorological station where they were recorded. Thresholds were not obtained for each station because, first, the DIAU station represents the urban climate in the city center, and second, the time series for the other stations are shorter than the 16-year available for the DIAU station. Using these criteria, the heatwaves shown in Table VII

Table V. Linear models (significance level of 0.005) applied to impute missing temperature data.

Stations	Model	Coefficient of determination (%)	Standard error of estimate (ºC)
Lomas del Mármol (*y*) vs. DIAU (*x*)	*y = 1.0671x - 1.7659*	97	0.90
Azumiatla (*y*) vs. DIAU (*x*)	*y = 1.0258x – 1.8889*	94	1.43
El Ameyal (*y*) vs. Azumiatla (*x*)	*y = 1.0117x +0.1440*	94	1.26
Resurrección (*y*) vs. El Ameyal (*x*)	*y = 0.9203x – 0.0563*	95	1.13

Table VI. Linear models (significance level of 0.005) applied to impute missing data for relative humidity.

Stations	Model	Coefficient of determination (%)	Standard error of estimate (percentage points)
Lomas del Mármol (*y*) vs. DIAU (*x*)	*y= 0.9024x + 1.0313*	89	5.3
Azumiatla (*y*) vs. DIAU (*x*)	*y= 1.2964x – 5.0465*	88	7.9
El Ameyal (*y*) vs. Azumiatla (*x*)	*y= 1.2424x + 8.7529*	87	7.2
Resurrección (*y*) vs. El Ameyal (*x*)	*y= 1.0161x + 3.3851*	88	10.8

Table VII. Heatwaves selected for this analysis.

Identifier	Dates	Station with the longest duration
I	March 22 to April 8, 2023	Lomas del Mármol
II	April 24 to May 8, 2023	DIAU and Lomas del Mármol
III	June 8 to 24, 2023	DIAU and Lomas del Mármol
IV	February 20 to 29, 2024	DIAU and Lomas del Mármol
V	March 7 to 24, 2024	Lomas del Mármol
VI	April 12 to 21, 2024	DIAU and Lomas del Mármol
VII	April 24 to June 13, 2024	DIAU and Lomas del Mármol

were selected, although some were limited to a single season or with interruptions in warm periods that do not allow a continuous wave to be configured.

The intensity of the heatwaves, expressed in degree-days of the waves, was calculated with the following procedure: for daytime heatwaves, the threshold T_{x90} corresponds to the 90th percentile of the daily maximum temperatures in the 2008-2023 series from the DIAU station, provided it is sustained for five consecutive days; similarly, T_{n90} was determined for daily minimum temperatures, serving as the threshold for nocturnal heatwaves (all the temperatures are expressed in ºC).

The intensity of the diurnal heatwave (*HWD*) was calculated according to the index proposed by Chen and Li (2017):

$$HWD = \sum_{i=1}^{duration} T_{xi} - T_{x90}, \forall T_{xi} > T_{x90} \quad (2)$$

where T_{xi} is the daily maximum temperature during the wave.

The intensity of the nocturnal heatwave (*HWN*) was:

$$HWN = \sum_{i=1}^{duration} T_{ni} - T_{n90}, \forall T_{ni} > T_{n90} \quad (3)$$

where T_{ni} is the daily minimum temperature during the wave. Accordingly, the intensity of the circadian heatwave (*HWC*), in degree-days, was:

$$HWC = HWD + HWN \quad (4)$$

for dates in which $HWD \neq 0$ and $HWN \neq 0$.

To evaluate the intensity in degree-hours, daily temperature data were used, assuming that the daily occurs around 15:00 LT, taken as the thermal noon for practical purposes. The daytime period was defined as six hours before and after 15:00 LT, that is, from 9:00 to 21:00 LT. Then, the diurnal period was defined as 9:00 to 20:00 LT, and the nocturnal period as 21:00 to 8:00 LT.

The intensity of the diurnal heatwave in degree-hours:

$$\{HWD\} = \sum_{j=9}^{20hours} T_j - T_{x90}, \quad (5)$$

for every hourly temperature T_j between 9:00 and 20:00 LT greater than T_{x90}.

The intensity of the nocturnal heatwave in degree-hours:

$$\{HWN\} = \sum_{j=21}^{8hours} T_j - T_{n90} \quad (6)$$

for every hourly temperature T_j between 21:00 and 8:00 LT greater than T_{n90}. The circadian sum of the heatwave in degree-hours was $\{HWC\} = \{HWD\} + \{HWN\}$, for dates in which $\{HWD\} \neq 0$ and $\{HWN\}$

4.1 Human bioclimate and heatwaves

To incorporate people's acclimatization, the preferred daytime and nighttime temperatures for the April-October semester were calculated using the equation developed by Morgan and Gómez-Azpeitia (2018) from survey applications (8018 questionnaires) across 13 cities in Mexico, contrasted with measurements of the ambient temperature to which respondents were exposed. The maximum preferred temperature (T_{PD}) was:

$$T_{PD} = 0.5\overline{T_x} + 13.1 \quad (7)$$

where $\overline{T_x}$ is the average maximum temperature of the DIAU station for the period 2008-2023. The minimum preferred temperature (T_{PN}) was:

$$T_{PN} = 0.5\overline{T_n} + 13.1 \quad (8)$$

where $\overline{T_n}$ is the average minimum temperature of the DIAU station from the period 2008-2023.

The above preferred temperatures were then used to calculate the preferred diurnal (H_{PD}) and nocturnal (H_{PN}) Humidex values (Cvijanovic et al., 2023) with the corresponding vapor pressures in hPa at 50% relative humidity (e_{50}):

$$H_{PD} = T_{PD} + \frac{5}{9}(e_{50} - 10) \quad (9)$$

$$H_{PN} = T_{PN} + \frac{5}{9}(e_{50} - 10) \quad (10)$$

The vapor pressure (e, measured in hPa) was calculated by solving the definition of relative humidity in tenths, as the quotient of the vapor pressure e between the saturation vapor pressure, e_s, this last one calculated from the temperature T (ºC) with the polynomial of Adem (1967):

$$e_s = b_{0+} + b_i\overline{T}^i \quad (11)$$

with = 6.115, = 0.42915, = 1.4205×10^{-2}, = 3.046×10^{-4}, = 3.2×10^{-6}

The diurnal bioclimatic discomfort in degree-hours was calculated using the Humidex ‹*HWD*› for every H_j greater than H_{PD}:

$$\langle HWD \rangle = \sum_{j=9}^{20hours} H_j - H_{PD} \quad (12)$$

Similarly, for the nocturnal, for every H_j greater than H_{PN}:

$$\langle HWN \rangle = \sum_{j=21}^{8hours} H_j - H_{PN} \quad (13)$$

And for the circadian period:

$$\langle HWC \rangle = \langle HWD \rangle + \langle HWN \rangle \quad (14)$$

A flowchart summarizing the methodology described above is shown in Figure 4.

The current mathematical expression of the Humidex bioclimatic index was introduced by Masterton and Richarson (1979). Like many other indices, it integrates the effect of humidity and atmospheric temperature on human thermal sensation (Gosling et al., 2014). Humidex is officially used by the Meteorological Service of Canada and has recently been applied for heatwave studies on a global or regional scale (Hamdi et al., 2016; Lee et al., 2016; Stewart et

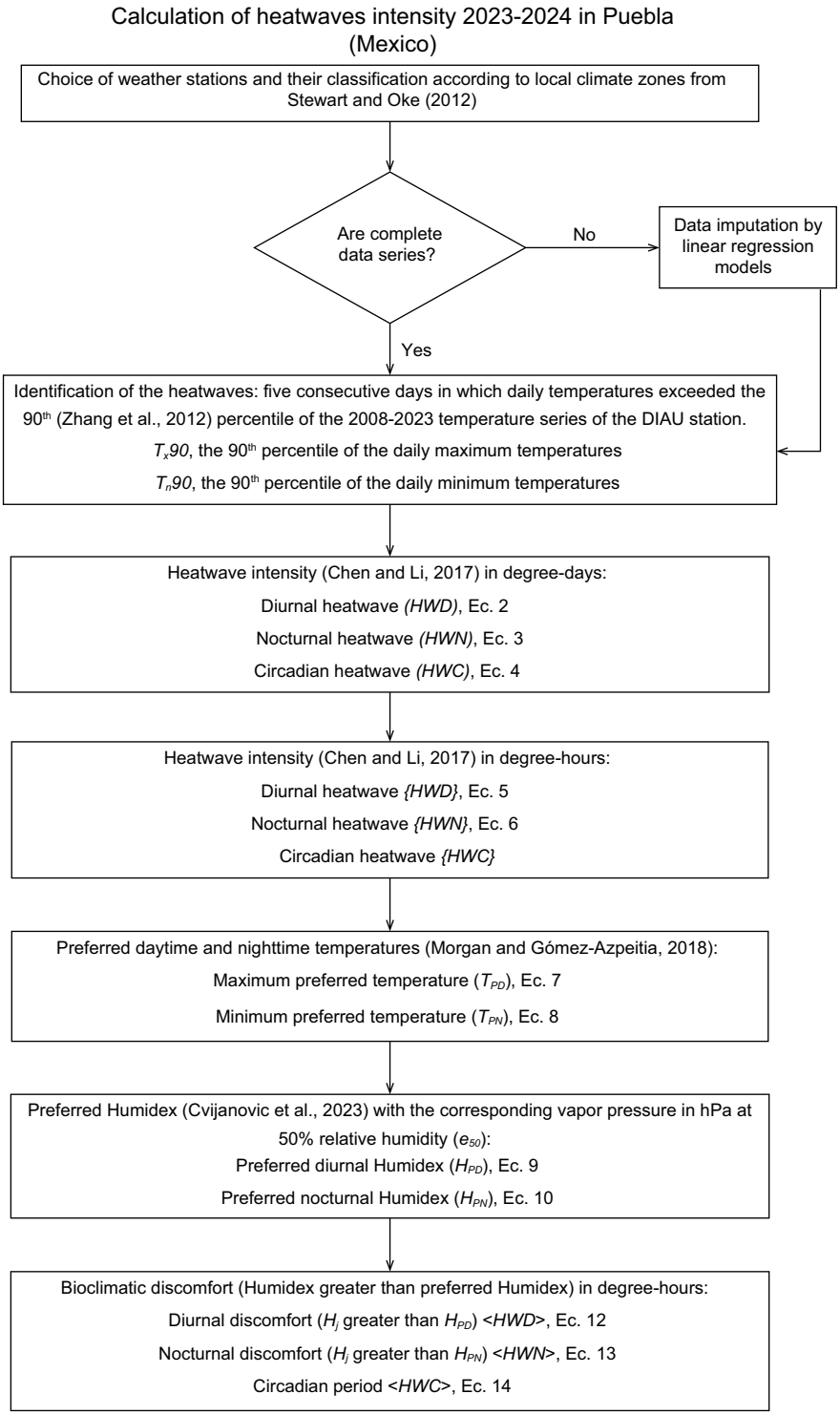

Fig. 4. Flowchart of the calculation of heatwave intensities in 2023 and 2024 in the city of Puebla. Own elaboration.

al., 2017; Heo and Bell, 2019; Neethu and Ramesh, 2022; Jeong et al., 2024; Półrolniczak, 2024); in urban climatology (Roshan et al., 2017; Geletič et al., 2018), and in the energy sector (Miller et al., 2017; Yildiz et al., 2017).

It must be added that since Humidex only depends on two variables, temperature and humidity, its calculation is simple. However, it does not incorporate the main factors affecting thermal stress, such as wind and mean radiant temperature. Despite this limitation, its main advantage compared to more complex indices (e.g., the universal thermal climate index [UTCI, see volume 56 of the International Journal of Biometeorology, 2012, entirely dedicated to this index] and the physiological equivalent temperature [PET; Höppe, 1999; Cimillo, 2020] lies in the high accessibility of the calculation data for Humidex, that is in situ air temperature and humidity measurement in contrast to mean radiant temperature usually calculated from another sub-model, as pointed by Geletič et al. (2018). In addition, the preferential use of Humidex enabled it to be adapted to Puebla conditions.

5. Results and discussion

Temperature differences between an urban site and its surroundings, and their relationship with heatwaves, show contrasting results in various studies. For example, an average decrease of 0.3 ºC during heatwaves, both during the day and at night, has been observed in 89 cities across India (Kumar and Mishra, 2019). In contrast, Pyrgou et al. (2020) reported an increase of 0.9-1.3 ºC during the daytime over an eight-year period in Nicosia, Cyprus. Other studies have even found no significant changes in the magnitude of the thermal contrast during heatwave events (Chew et al., 2021; Richard et al., 2021).

Figures 5 to 7 show these differences for the year 2023 between the urban station (DIAU) and the other four stations listed in Table I, using the imputation procedure described in the data section. Between DIAU and Lomas del Mármol, the temperature differences (Fig. 5) are predominantly positive, except from midday to sunset. In the case of Azumiatla, negative differences occur from dawn to noon but only during the warm semester. Against El Ameyal, these negative differences extend from dawn to early afternoon, between April and December. Throughout the rest of the year, practically all the differences are positive, with more pronounced values during nighttime. On the other hand, when compared with Resurrección, negative differences are less frequent, but it must be considered that between the DIAU station and El Ameyal there is a 200 m difference in elevation.

The differences in relative humidity (Fig. 6) result from the inverse behavior between this variable and air temperature; therefore, it is more relevant to analyze the contrasts in absolute humidity (Fig. 7). At the DIAU station, a higher water vapor content was observed most of the time, except for the last three months of the year—before noon and near sunset—when compared to the Lomas del Mármol. In contrast with the other three stations, DIAU showed higher vapor levels throughout the entire diurnal cycle.

The Humidex bioclimatic index assesses the feeling of comfort by combining air temperature and atmospheric humidity through vapor pressure. Figure 8 shows that most of the time this sensation is "warmer" (or "less cold") at the DIAU than at the rest of the seasons, except for some short periods: the last four months of the year from noon to sunset when compared to Lomas del Mármol; the early morning hours in the warm semester when compared to Azumiatla; and the same from April to the rest of the year when contrasted to El Ameyal and Resurrección. The higher Humidex values observed at the DIAU station will be reflected in the assessment of heatwave intensities, as will be shown later.

Figure 9 compares the diurnal intensities of the seven heatwaves analyzed, expressed in degree-days and calculated according to the procedure described in Eqs. (2), (3), and (4), based on the daily maximum and minimum temperatures. The Lomas del Mármol station (LCZ 2_b) maintains the highest values during the seven diurnal waves (Fig. 9a), while Resurrección (LCZ 9), located on average 200 m higher than the others, showed the lowest values. On the other hand, for nocturnal (Fig. 9b) and circadian waves (Fig. 9c), the DIAU station reaches the highest values. A similar pattern is observed when comparing the Azumiatla (LCZ C_9) and El Ameyal (LCZ D_6) stations: in the diurnal waves, the latter surpasses the former, whereas in the nocturnal and circadian waves, their values are very similar.

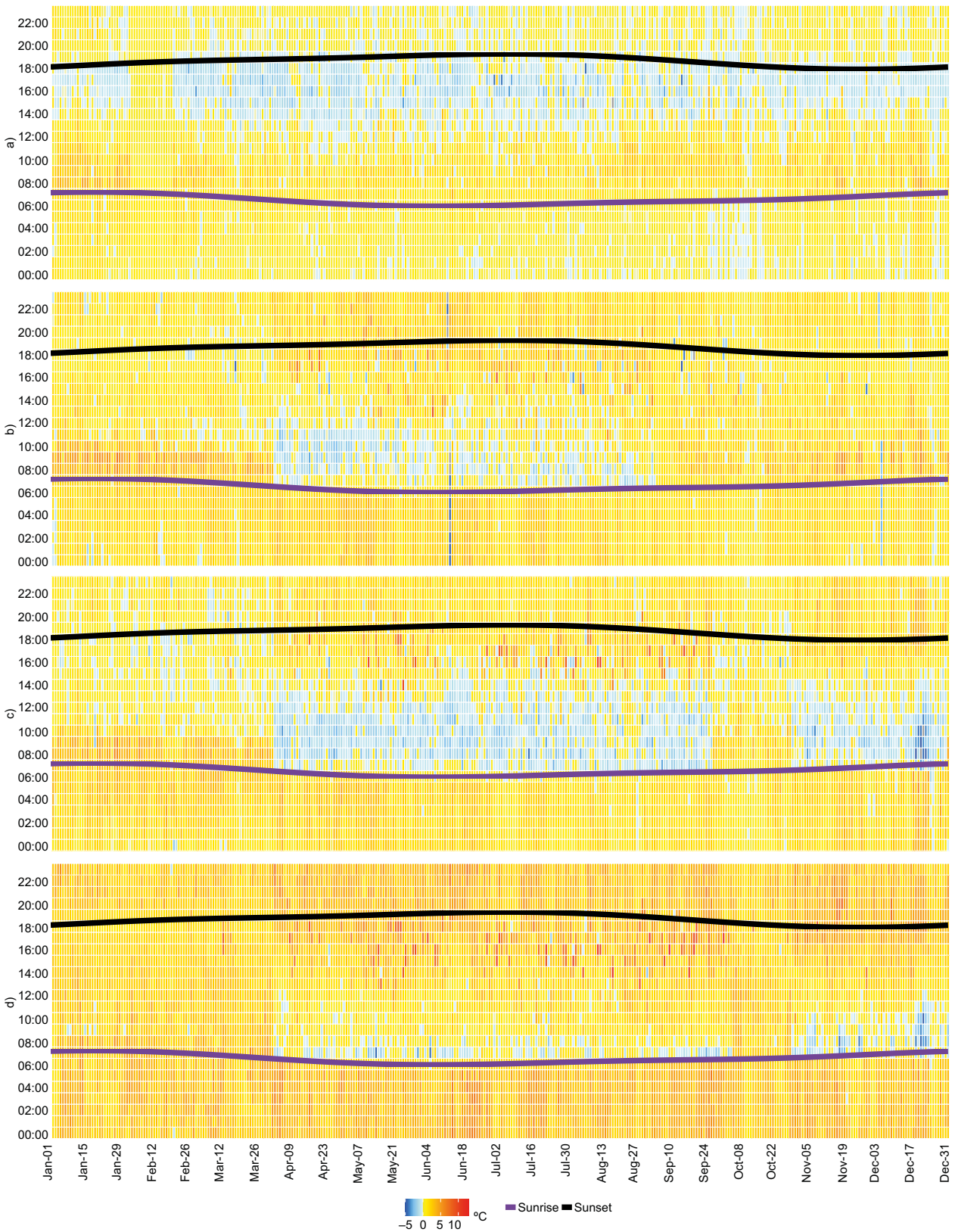

Fig. 5. Temperature differences for the year 2023 between the DIAU stations and: (a) Lomas del Mármol (ranging from –5.4 to 5.6 ºC, with an average of 0.5 ºC); (b) Azumiatla (–6.2 to 8.7 ºC, average 1.4 ºC); (c) El Ameyal (–6.1 to 10.8 ºC, average 1.1 ºC); (d) Resurrección (–6.1 to 10.8 ºC, average 1.1 ºC). Days of the year are shown on the *x*-axis and local time on the *y*-axis.

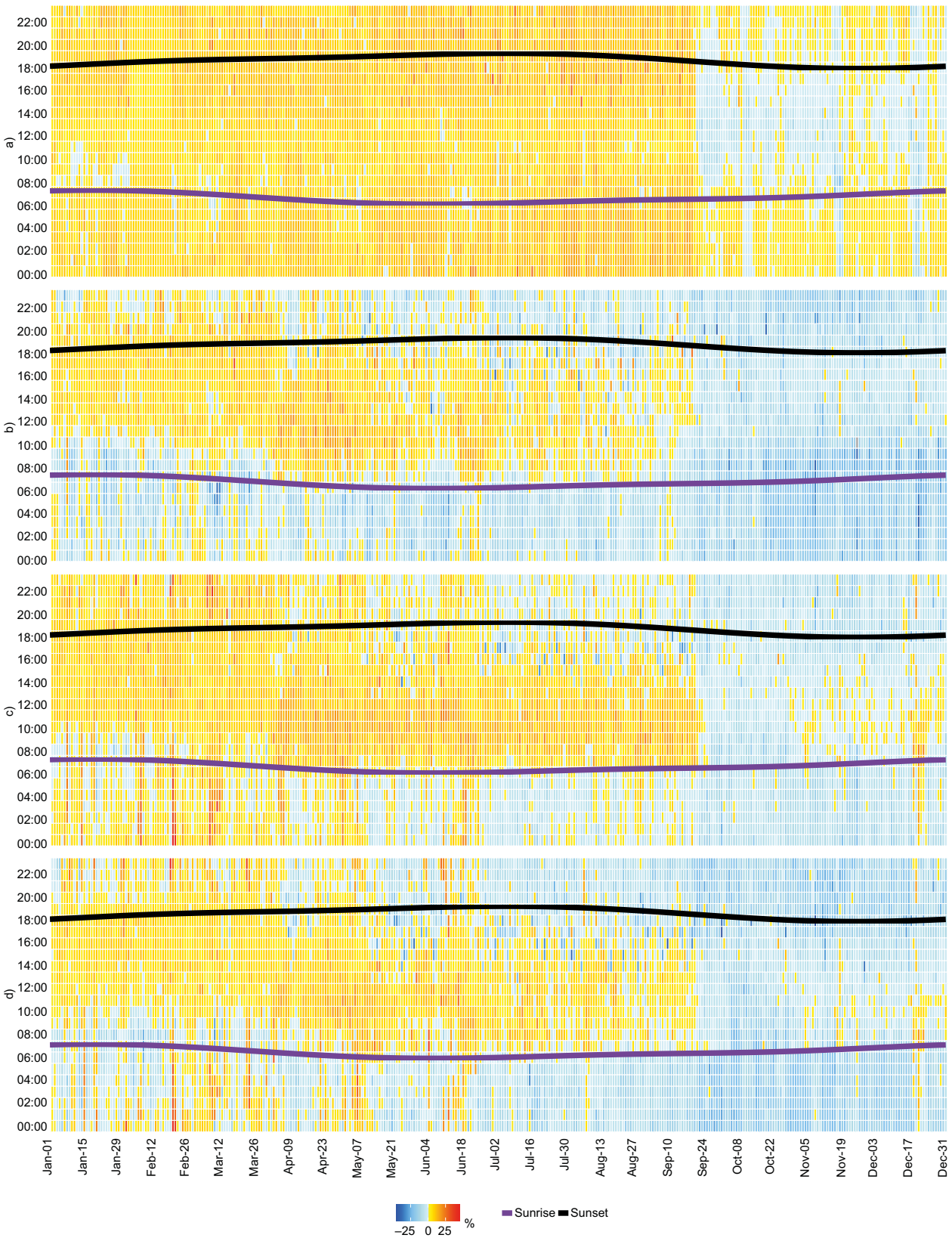

Fig. 6. Differences in relative humidity for the year 2023 in percentage points, between the DIAU stations and: (a) Lomas del Mármol (ranging from –25 to 30, with an average of 6); (b) Azumiatla (–48 to 32, average –4); (c) El Ameyal (–34 to 48, average of 1); (d) Resurrección (–46 to 45, average 3). Days of the year are shown on the *x*-axis and local time on the *y*-axis.

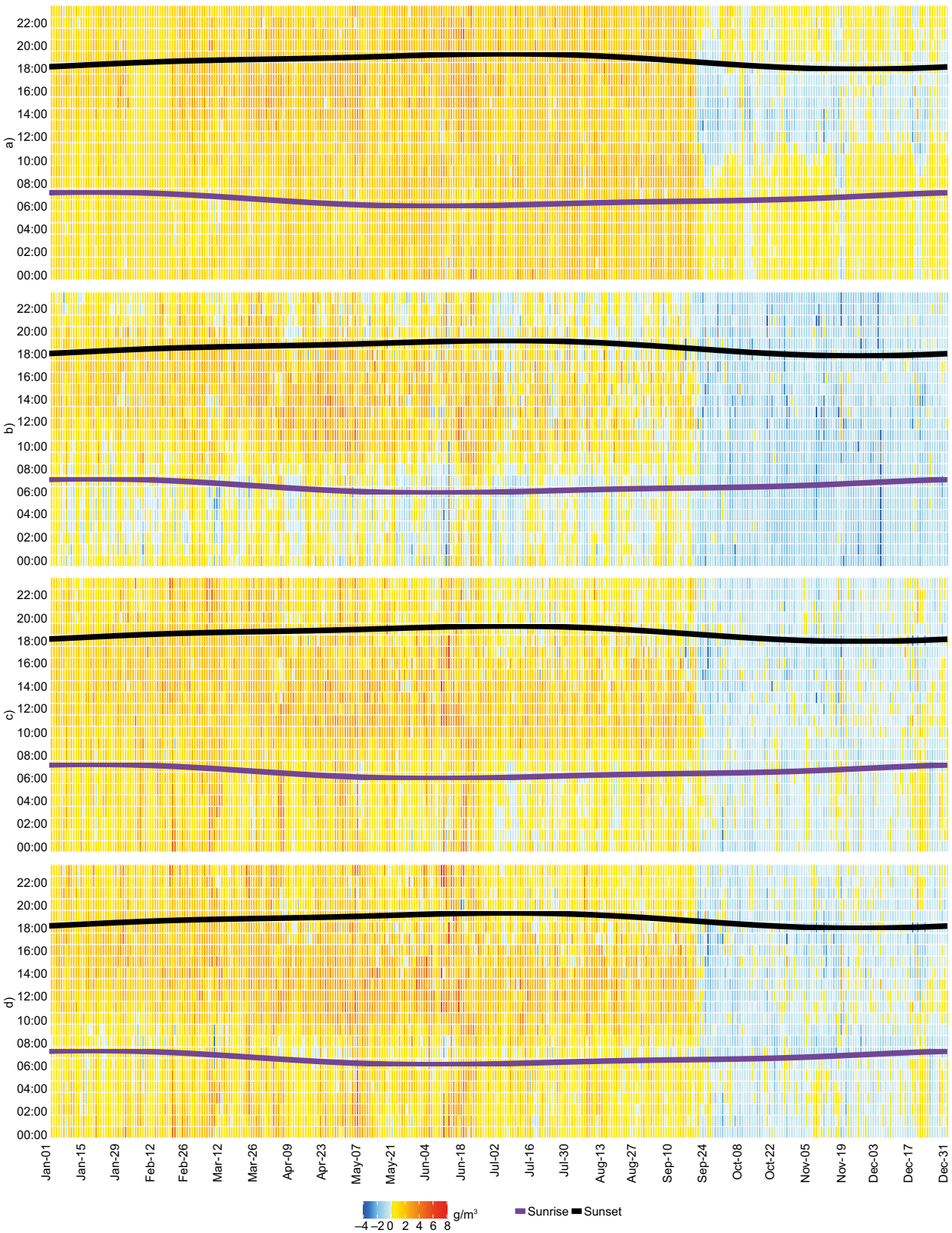

Fig. 7. Differences in absolute humidity in g m^{-3} for the year 2023, between the DIAU stations and: (a) Lomas del Mármol (ranging from –3.1 to 5.1, with an average of 1.2); (b) Azumiatla (–8.1 to 5.2, average of 0.3); (c) El Ameyal (–3.5 to 7.8, average of 0.8); (d) Resurrección (–3.5 to 7.6, average of 0.9). Days of the year are shown on the *x*-axis and local time on the *y*-axis.

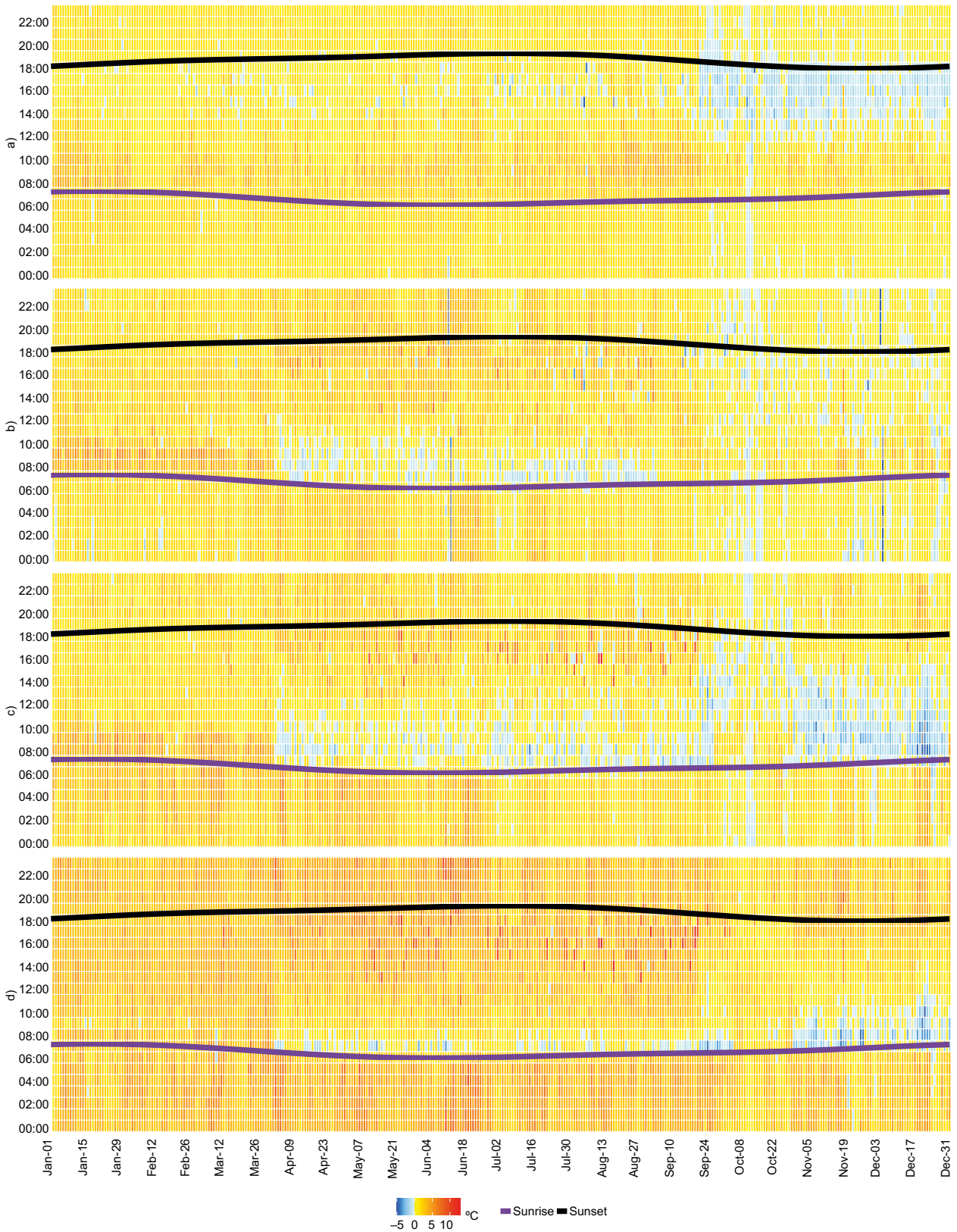

Fig. 8. Differences in the Humidex bioclimatic index in ºC for the year 2023, between the DIAU stations and: (a) Lomas del Mármol (ranging from –5.0 to 5.8, with an average of 1.4); (b) Azumiatla (–11.6 to 9.0, average of 1.7); (c) El Ameyal (–6.0 to 13.1, average of 1.7); (d) La Resurección (–4.6 to 13.0, average of 3.2). Days of the year are shown on the *x*-axis and local time on the *y*-axis.

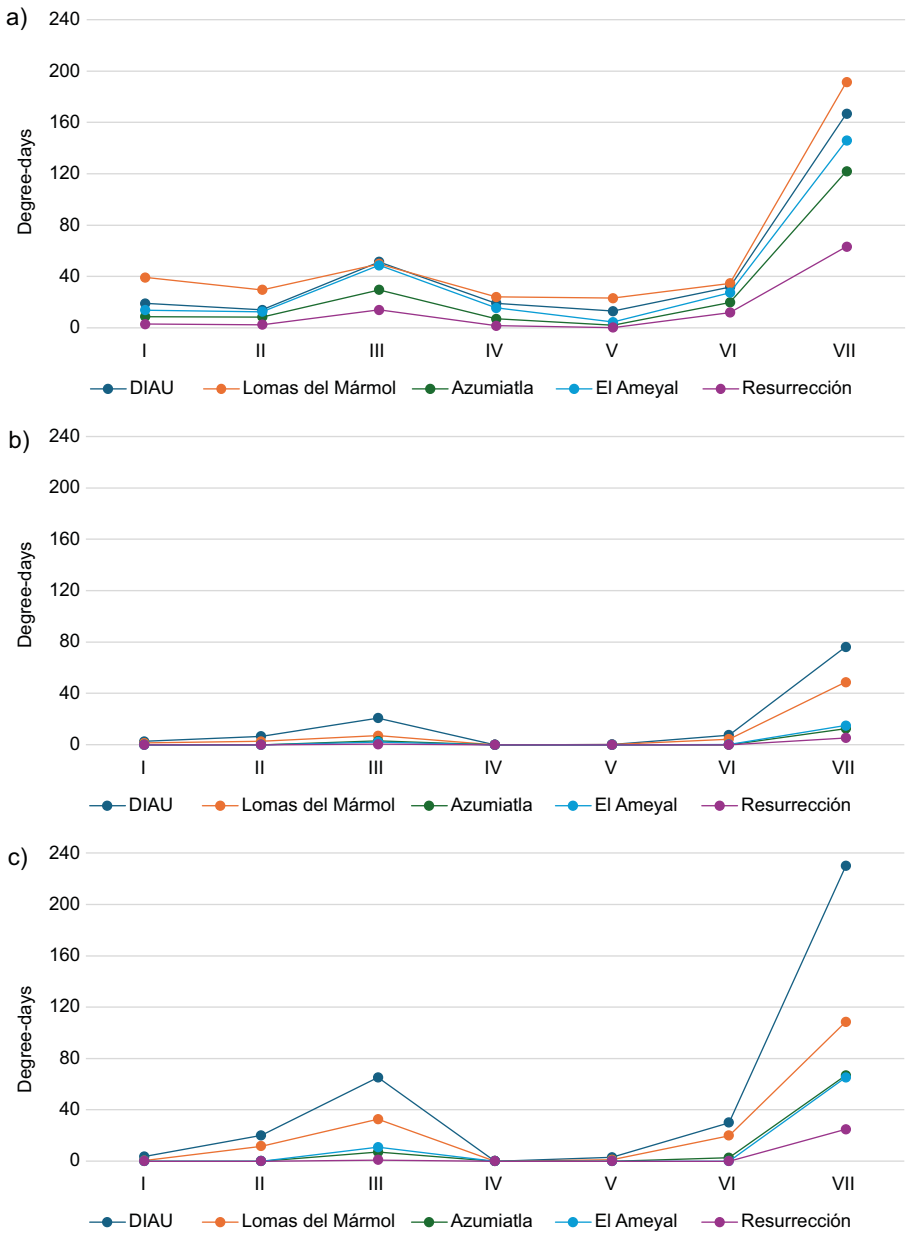

Fig. 9. Heatwave intensities in degree-days (Y-axis). The X-axis shows the keys (see Table VII) to each wave: (a) diurnal, (b) nocturnal, (c) circadian sum.

Evaluated in degree-days and applying the criterion of at least five consecutive days in which daily temperatures exceed the 90th percentile—determined from the 2008-2023 series at the DIAU station, which resulted in 27.4 ºC for maximum temperatures and 17.4 ºC for minimum temperatures—the two most intense waves among the seven analyzed (III, from June 8 to 24, 2023, and VII, from April 24 to June 13, 2024) at Lomas del Mármol or in the DIAU are approximately 1.5 times more intense than at Azumiatla and El Ameyal, and at least three times more intense than at Resurrección. Evidently, wave VII, due to its duration of 50 days, was three times as intense as wave III, which lasted 17 days.

Figure 10 was obtained by applying Eqs. (5), (6), and (7) to the highest temperatures of each hour. As

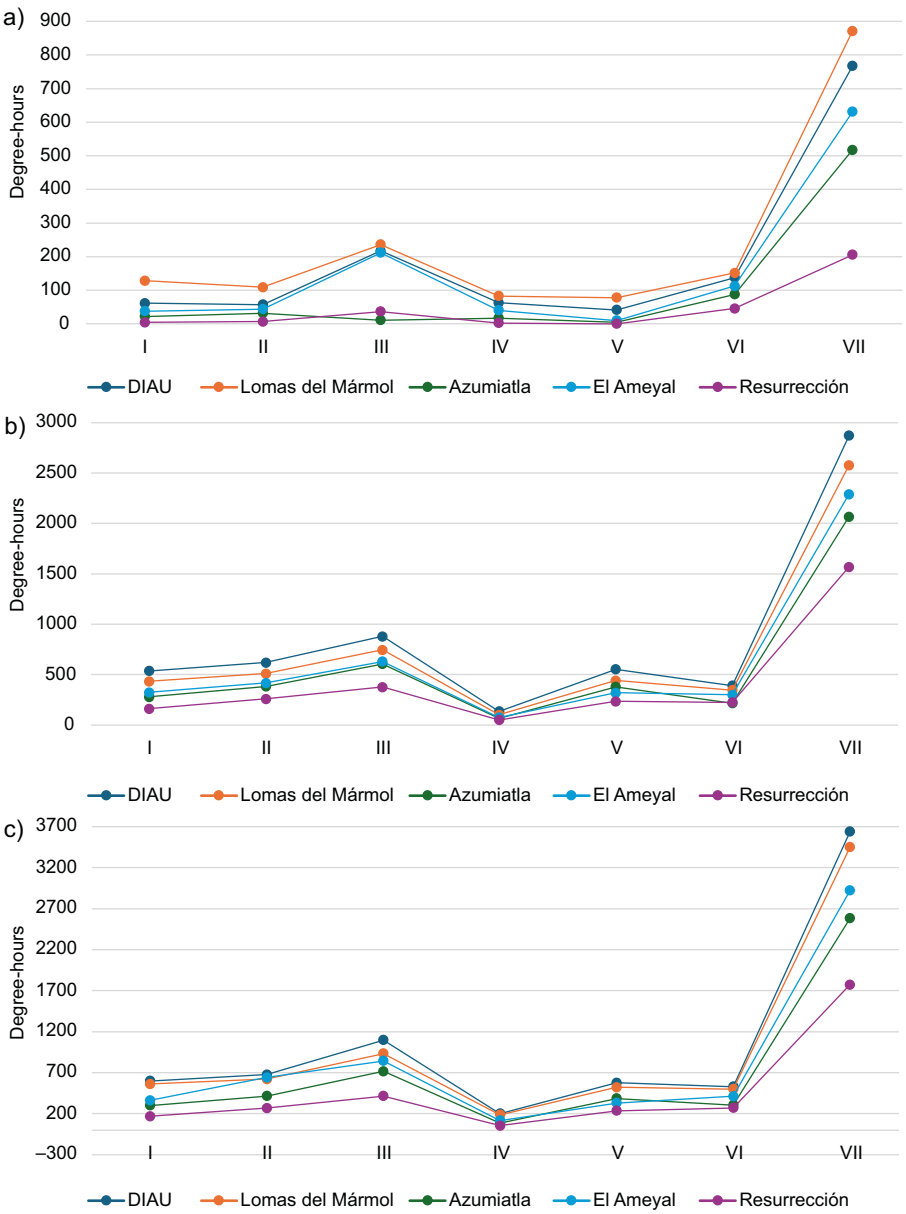

Fig. 10. Heatwave intensities in degree-hours (*y*-axis). The *x*-axis shows the keys (see Table VII) to each wave: (a) diurnal, (b) nocturnal, (c) circadian sum.

already said, the diurnal period was considered from 9:00 to 20:00 LT, while the nocturnal period is from 21:00 to 8:00 LT. Intensities are in degree-hours. In general, the same proportions are maintained between the stations that were described for Figure 9 but, as analyzing hourly data gains in temporal resolution, the nocturnal components of waves IV (February 20 to 29, 2024) and V (March 7 to 24, 2024), which are not detected in degree-days (Fig. 9b), now do appear (Fig. 8b) and, similarly, for the circadian sums in degree-hours (Fig. 10c).

The predominance of the DIAU station during the night periods in Figures 9 and 10 can be well explained by the nocturnal heat island effect evident in the temperature contrast maps of Figure 5.

Figure 11 evaluates the intensity of the waves incorporating the effect of atmospheric humidity through the Humidex index, and the acclimatization

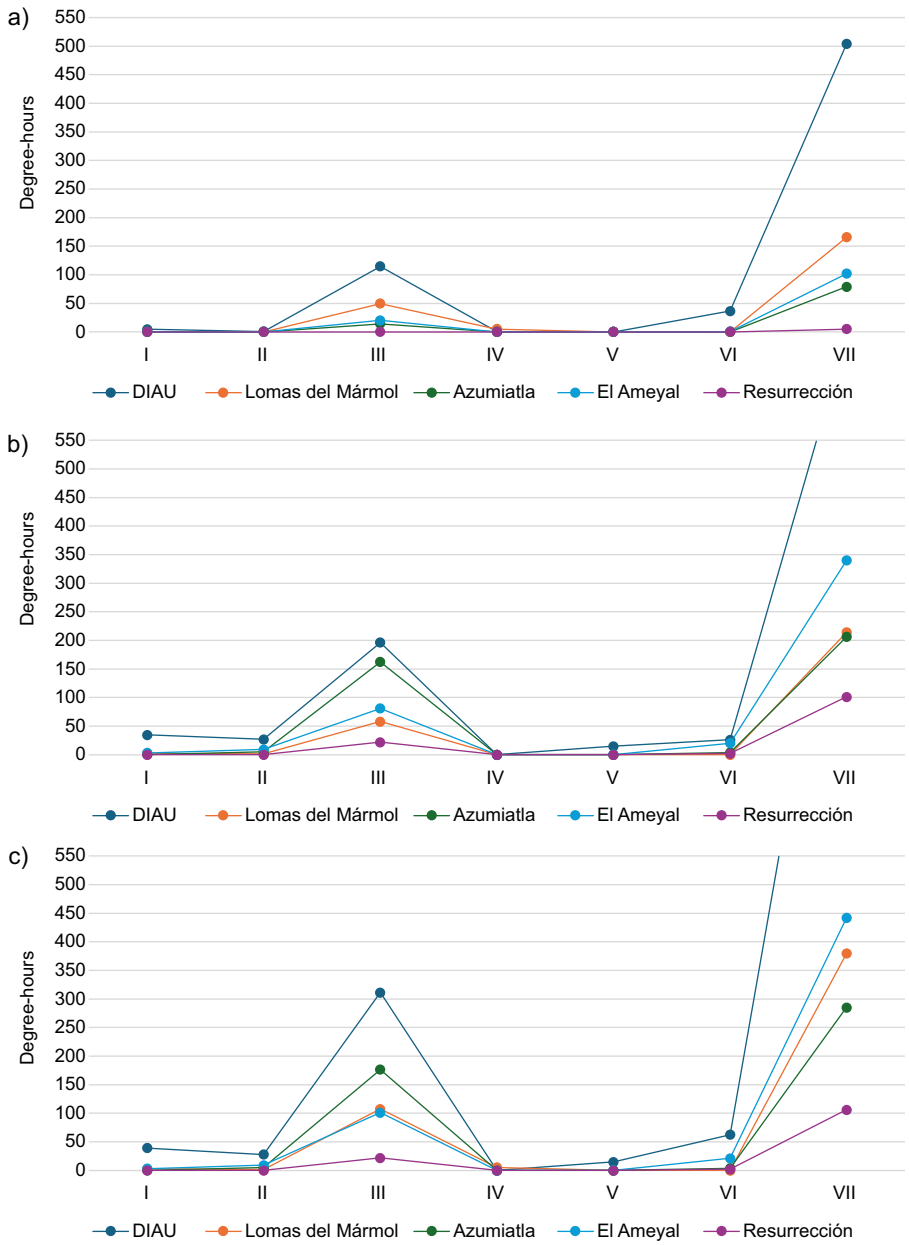

Fig. 11. Heatwave intensities in degree-hours over the preferred Humidex value (*y*-axis). The *x*-axis shows the keys (see Table VII) to each wave: (a) diurnal, (b) nocturnal, (c) circadian sum.

of the population as indicated in Eqs. (7), (8), (9), and (10), completing the procedure with Eqs. (11), (12), (13), and (14). Thus, the degree-hours in which the Humidex was above diurnal or nocturnal comfort (between 9:00 and 20:00 LT or between 21:00 and 8:00 LT, respectively) are obtained, considering that said comfort is achieved with the thermopreferendum of the May-October period of the DIAU 2008-2023 series, applying Eqs. (7) and (8), with a relative humidity of 50% (Table VIII). The results are attenuated by the relatively low values of relative humidity during these seven waves (ranging from 30 to 45%). It is notable that the conditions only deviate noticeably from the comfort Humidex

Table VIII. Preferred values (ºC) for the May-October period in the 2008-2023 series of the DIAU station.

Variable	Maximum	Minimum
Average temperature	24.9	14.2
Preferred temperature	25.5 (Eq. 7)	20.2 (Eq. 8)
Preferred Humidex	29.0 (Eq. 9)	21.2 (Eq. 10)

during the two most intense waves of the set of seven studied, but for both the diurnal and nocturnal periods there is a predominance of the DIAU station, which doubles Lomas del Mármol for wave III (June 8 to 24, 2023), but quadruples this same station for wave VII (April 24 to June 13, 2024) due to the effect of atmospheric humidity (see maps of absolute humidity contrasts in Fig. 7 and Tejeda-Martínez et al. [2023]) because the DIAU station is located near green areas, as shown in Figure 2, mainly parks and urban corridors with Indian laurel trees, jacarandas, eucalyptus, bougainvilleas, Peruvian peppertrees, pines, and date palms (Gómez-Martínez et al., 2021).

6. Conclusions

The heatwaves of 2023 and 2024 were exceptional in Mexico and affected cities that had rarely experienced such events. This study analyzes the changes across different areas of Puebla. The identification of these differential patterns contributes to the understanding of urban heat dynamics and thus provides a transferable framework for comparative analyses in other metropolitan contexts.

It was found that nocturnal waves in the city center are more intense—due to the urban heat island—and that, in LCZ with greater vegetation, the intensity of heatwaves increases when the contribution of atmospheric humidity is incorporated into their evaluation.

Heatwaves are accentuated at night by the UHI. In Mexico City, Luyando-López (2016) found that heatwaves generate less mortality than cold waves. This highlights the need to understand the contrasting impacts of thermal extremes in different regions and underscores the relevance of assessing urban vulnerability to both heat and cold waves.

As indicated in the Methodology section, the evaluation of heatwave intensities from hourly temperatures showed greater precision compared to the procedure that uses only daily temperatures. The use of Humidex and the incorporation of acclimatization through the preferred diurnal and nocturnal temperatures of the May-October period, although it attenuates the results, show the predominant behavior of the DIAU station over the others, both during the day and at night, due to the higher ambient humidity of its surroundings compared to the other four. It must be noted that the procedure shown here can also be applied to different atmospheric conditions of temperature and humidity, such as to evaluate the intensity of cold or heatwaves, whether humid or dry.

Climate change indices for the DIAU station show an increasing trend in temperature, but this study did not evaluate trends in the intensity and frequency of heatwaves in Puebla. However, the occurrence of heat waves in the non-warm seasons of the year is striking, such as wave I in the first days of spring 2023 and wave IV in the final days of the winter period 2023-2024.

Through the results obtained from the seven cases analyzed, it is possible to conclude that, at a regional level for Puebla, heatwaves have a more marked presence from middle to late spring and, at the same time, there is an influence of land use or urban/natural elements on comfort, since in the DIAU station, both in nocturnal and diurnal heat waves, the degree-hours above the preferred Humidex were always higher compared to the other four stations, where there is more natural vegetation and small buildings. These findings, together with the proposed methodology, could support decision-makers in developing early warning systems to advise populations on avoiding specific urban areas during heatwave events or periods of extreme temperatures. This study identifies zones with an "excess of degrees", thereby providing valuable information to improve public awareness and planning during such events.

The calculations of degree-days and degree-hours, in addition to improving the precision of the waves' intensity, can be the basis for future proposals on mitigation or studies on exposure to heat and its associated health problems, such as mortality or morbidity (Anderson and Bell, 2011; Sung et al., 2013) due to thermal stress, heat stroke, and cardiovascular diseases (Michelozzi et al., 2009), among others.

The methodology proposed in this study aims to contribute to local and global efforts to improve urban heat assessment in developing cities, where intra-urban thermal heterogeneity and the health impacts of extreme heat remain largely unexplored (Campbell et al., 2018). This approach is intentionally simple, relying solely on readily available variables such as temperature and atmospheric humidity, given the frequent lack of comprehensive meteorological data, particularly in many Latin American contexts.

Acknowledgments

To Omar Castro Díaz and René Gómez Díaz from the Grupo de Climatología Aplicada of the Universidad Veracruzana, for the calculations and preparation of figures. To Talía Ramírez-González, from the DIAU, for the generation of images to characterize the local climatic zones of the analyzed meteorological stations. This paper is part of the PAPIIT IN107123 UNAM project "Analysis of the urban bioclimate and possible adaptation actions in the face of the observed and projected changes in the city of Puebla".

References

Adem J. 1967. Parameterization of atmospheric humidity using cloudiness and temperature. Monthly Weather Review 95: 83-88. https://doi.org/10.1175/1520-0493(1967)095<0083:POAHUC>2.3.CO;2

Alejo-Sánchez LE, Márquez-Grajales A, Salas-Martínez F, Franco-Arcega A, López-Morales V, Acevedo-Sandoval OA, González-Ramírez CA, Villegas-Vega R. 2025. Missing data imputation of climate time series: A review. MethodsX: 103455. https://doi.org/10.1016/j.mex.2025.103455

Anderson GB, Bell ML. 2011. Heat waves in the United States: Mortality risk during heat waves and effect modification by heat wave characteristics in 43 US communities. Environmental Health Perspectives 119: 210-218. https://doi.org/10.1289/ehp.1002313

Balderas-Romero G, Mayorga-Rapozzo R, Méndez-Spíndola R. 2009. Implicaciones climatológicas de la metropolización en el Valle de Puebla. Technical report. BUAP, Fondo Mixto, CONACYT, Gobierno del Estado de Puebla, 104 pp.

Balderas-Romero G. 2018. Efectos climáticos de la urbanización en la zona metropolitana de Puebla. In: Ambiente urbano 2050 (Santillán-Soto N, García-Cueto OR, Eds.). Universidad Autónoma de Baja California, Mexicali, Baja California, México, 69-95.

Boni Z, Bieńkowska Z, Chwałczyk F, Jancewicz B, Marginean I, Serrano PY. 2023. What is a heat(wave)? An interdisciplinary perspective. Climatic Change 176: 129. https://doi.org/10.1007/s10584-023-03592-3

C3S. 2025. The 2024 annual climate summary. Global climate highlights 2024. Programme of the European Union-Copernicus, Climate Change Service-ECMWF. Available at: https://climate.copernicus.eu/sites/default/files/custom-uploads/GCH-2024/GCH2024-PDF-1.pdf (accessed 2025 February 5)

Campbell S, Remenyi TA, White CJ, Johnston FH. 2018. Heatwave and health impact research: A global review. Health & Place 53: 210-218. https://doi.org/10.1016/j.healthplace.2018.08.017

CENAPRECE. 2024. Temporada de calor, prevención y atención de daños a la salud, 2024. Secretaría de Salud-Centro Nacional de Programas Preventivos y Control de Enfermedades. Available at: https://www.gob.mx/cms/uploads/attachment/file/903561/TEMPORADA_DE_CALOR__2024_FINAL__2_.pdf (accessed 2024 October 24)

Chen Y, Li Y. 2017. An inter-comparison of three heatwave types in China during 1961-2010: Observed basic features and linear trends. Scientific Reports 7: 45619. https://doi.org/10.1038/srep45619

Cheng S, Wang S, Li M, He Y. 2024. Summer heatwaves in China during 1961-2021: The impact of humidity. Atmospheric Research 304: 107366. https://doi.org/10.1016/j.atmosres.2024.107366

Chew LW, Liu X, Li XX, Norford LK. 2021. Interaction between heat wave and urban heat island. A case study in a tropical coastal city: Singapore. Atmospheric Research 247: 105134. https://doi.org/10.1016/j.atmosres.2020.105134

Cimillo M. 2020. PET Physiological Equivalent Temperature–La valutazione del comfort termico in ambienti esterni. In: Adapting to the changing climate: Knowledge innovation for environmental design (Losasso M, Lucarelli MT, Rigillo M, Valente R, Eds.). Maggioli Editore, Milano.

CONABIO. 2024. Geoportal del Sistema Nacional de Información sobre Biodiversidad. Comisión Nacional para el Conocimiento y Uso de la Biodiversidad, México. Available at: http://www.conabio.gob.mx/informacion/gis/ (accessed 2024 December 1).

CONAGUA. 2024a. Reporte anual del clima en México 2023. Coordinación General del Servicio Meteorológico Nacional, Comisión Nacional del Agua, México. Available at: https://smn.conagua.gob.mx/tools/DATA/Climatolog%C3%ADa/Diagn%C3%B3stico%20Atmosf%C3%A9rico/Reporte%20del%20Clima%20en%20M%C3%A9xico/Anual2023.pdf (accessed 2024 December 9)

CONAGUA. 2024b. Reporte del clima en México. Mayo 2024. Coordinación General del Servicio Meteorológico Nacional, Comisión Nacional del Agua, Mexico. Available at: https://smn.conagua.gob.mx/tools/DATA/Climatolog%C3%ADa/Diagn%C3%B3stico%20Atmosf%C3%A9rico/Reporte%20del%20Clima%20en%20M%C3%A9xico/RC-Mayo24.pdf (accessed 2024 November 14)

Cvijanovic I, Mistry MN, Begg JD. Gasparrini A, Rodó X. 2023. Importance of humidity for characterization and communication of dangerous heatwave conditions. npj Climate and Atmospheric Science 6: 33. https://doi.org/10.1038/s41612-023-00346-x

De Bono A, Peduzzi P, Giuliani G, Kluser S. 2004. Impacts of summer 2003 heatwave in Europe. UNEP/DEWA/GRID-Europe Environment Alert Bulletin 2: 1-4. Available at: https://www.unisdr.org/files/1145_ewheatwave.en.pdf (accessed 2024 November 6)

DGE. 2023. Temperaturas naturales extremas (temporada de calor 2023). Semana epidemiológica 40 (del 1 al 7 de octubre 2023). Dirección General de Epidemiología, Secretaría de Salud. Available at: https://www.gob.mx/cms/uploads/attachment/file/862593/TNE_SE_40.pdf (accessed 2024 October 24)

Flores-González S, Ladino-Álvarez RA. 2018. Riesgos naturales en el municipio de Puebla. Estudio de caso en Barranca Honda y Epazotlate. Montiel y Soriano Editores-Benemérita Universidad Autónoma de Puebla, México.

Gäb GM. 1970. Investigaciones del clima de la ciudad de Puebla. Revista Comunicaciones de la Fundación Alemana 17: 25-40.

Gäb GM. 1976. Untersuchungen zum Stadtklima von Puebla (Mexiko). Ph.D. thesis, Rheinischen Friedrich-Wilhelms- Universitat, Bonn.

Gálvez-Vidal J. 2021. Tendencias recientes de la humedad atmosférica ante el crecimiento urbano en Puebla, Puebla. B.Sc. in Atmospheric Sciences, Universidad Veracruzana.

Geletič J, Lehnert M, Savić S, Milošević D. 2018. Modelled spatiotemporal variability of outdoor thermal comfort in local climate zones of the city of Brno, Czech Republic. Science or The Total Environment 624: 385-395. https://doi.org/10.1016/j.scitotenv.2017.12.076

García-Cueto RO, Tejeda-Martínez A, Jáuregui-Ostos E. 2010. Heatwaves and heat days in an arid city in the northwest of Mexico: Current trends and in climate change scenarios. International Journal of Biometeorology 54: 335-345. https://doi.org/10.1007/s00484-009-0283-7

García-Martínez IM, Bollasina MA. 2021. Identifying the evolving human imprint on heatwave trends over the United States and Mexico. Environmental Research Letters 16: 094039. https://doi.org/10.1088/1748-9326/ac1edb

Gómez-Martínez F, de Beurs KM, Koch J. Widener J. 2021. Multi-temporal land surface temperature and vegetation greenness in urban green spaces of Puebla, Mexico. Land 10: 155. https://doi.org/10.3390/land10020155

Gosling SN, Lowe JA, McGregor GR, Pelling M, Malamud BD. 2009. Associations between elevated atmospheric temperature and human mortality: A critical review of the literature. Climatic Change 92: 299-341. https://doi.org/10.1007/s10584-008-9441-x

Gosling SN, Bryce EK, Dixon PG, Gabriel KMA, Gosling EY, Hanes JM, Hondula DM, Liang L, Bustos-Mac Lean PA, Muthers S, Nascimiento ST, Petralli M, Vanos JK, Wanka ER. 2014. A glossary for biometeorology. International Journal of Biometeorology 58: 277-308. https://doi.org/10.1007/s00484-013-0729-9

Hamdi R, Duchêne F, Berckmans J, Delcloo A, Vanpoucke C, Termonia P. 2016. Evolution of urban heatwave intensity for the Brussels Capital Region in the ARPEGE-Climat A1B scenario. Urban Climate 17: 176-195. https://doi.org/10.1016/j.uclim.2016.08.001

Heo S, Bell ML. 2019. Heat waves in South Korea: Differences of heat wave characteristics by thermal indices. Journal of Exposure Science & Environmental Epidemiology 29: 790-805. https://doi.org/10.1038/s41370-018-0076-3

Höppe P. 1999. The physiological equivalent temperature—A universal index for the biometeorological assessment of the thermal environment. International Journal of Biometeorology 43: 71-75. https://doi.org/10.1007/s004840050118

IMPLAN Puebla. 2016. Sistema de Información Geográfica Municipal SIGEM. Instituto Municipal de

Planeación de Puebla. Available at: https://sigemp.implanpuebla.gob.mx/ (accessed 2024 December 1)

INEGI. 2010. Compendio de información geográfica municipal 2010. Puebla. Instituto Nacional de Estadística y Geografía. Available at: https://www.inegi.org.mx/contenidos/app/mexicocifras/datos_geograficos/21/21114.pdf (accessed 2024 September 11)

INEGI. 2024. Anuario estadístico y geográfico por entidad federativa 2023. Aguascalientes. Instituto Nacional de Estadística y Geografía. Available at: https://www.inegi.org.mx/contenidos/productos/prod_serv/contenidos/espanol/bvinegi/productos/nueva_estruc/889463916376.pdf (accessed 2024 October 30)

IPCC. 2023. Summary for policymakers. In: Climate change 2023. Synthesis report. Contribution of working groups I, II and III to the Sixth Assessment Report of the Intergovernmental Panel on Climate Change (Core Writing Team, Lee H. and Romero J., Eds.). Geneva, Switzerland, 1-34. Available at: https://www.ipcc.ch/report/ar6/syr/downloads/report/IPCC_AR6_SYR_SPM.pdf (accessed 2024 November 10)

Jáuregui E. 1997. Heat island development in Mexico City. Atmospheric Environment 31: 3821-3831. https://doi.org/10.1016/S1352-2310(97)00136-2

Jáuregui E. 2000. El clima de la Ciudad de México. Instituto de Geografía de la UNAM-Plaza y Valdés, Ciudad de México.

Jáuregui E. 2009. The heat spells of Mexico City. Investigaciones Geográficas 70: 71-76.

Jeong DI, Yu B, Cannon AJ. 2024. 2021 heatwave over Western North America: Structural uncertainty and internal variability in GCM projections of Humidex and temperature extremes. Earth´s Future 12: e2024EF004541. https://doi.org/10.1029/2024EF004541

Kotsiantis S, Kostoulas A, Lykoudis S, Argiriou A, Menagias K. 2006. Filling missing temperature values in weather data banks. In: 2nd IET International Conference on Intelligent Environments (IE 06), Athens. https://digital-library.theiet.org/doi/abs/10.1049/cp%3A20060659 (accessed 2025 November 11)

Kumar R, Mishra V. 2019. Decline in surface urban heat island intensity in India during heatwaves. Environmental Research Communications 1: 031001. https://doi.org/10.1088/2515-7620/ab121d

Lee JS, Byun HR, Kim DW. 2016. Development of accumulated heat stress index based on time time-weighted function. Theoretical and Applied Climatology 124: 541-554. https://doi.org/10.1007/s00704-015-1434-x

Lemus-Flores S. 2016. Isla de calor en la ciudad de Puebla. B.Sc. thesis, Universidad Nacional Autónoma de México.

López-García AR. 2018. Modelación espacial del riesgo por calor extremo en el Área Metropolitana de Guadalajara, México. Revista Iberoamericana de Ciencias 5: 52-63.

Luyando-López E. 2016. Efectos de las temperaturas y precipitaciones extremas en el bioclima humano de la zona metropolitana de la ciudad de México por cambio climático local y global. Ph.D. thesis, Universidad Nacional Autónoma de México.

Marengo JA, Costa MC, Cunha AP, Espinoza JC, Jiménez, JC, Libonati R, Miranda V, Trigo IF, Sierra JP, Geirinhas JL, Ramos AM, Skansi M, Molina-Carpio J, Salina R. 2025. Climatological patterns of heatwaves during Winter and spring 2023 and trends for the period 1979-2023 in central South America. Frontiers in Climate 7: 1529082. https://doi.org/10.3389/fclim.2025.1529082

Martínez-Austria PF, Bandala ER, Patiño-Gómez C. 2016. Temperature and heat wave trends in northwest Mexico. Physics and Chemistry of the Earth, Parts A/B/C 91: 20-26. https://doi.org/10.1016/j.pce.2015.07.005

Masterton JM, Richarson FA. 1979. Humidex, a method of quantifying human discomfort due to excessive heat and humidity. Environment Canada, Ontario. Available at: https://publications.gc.ca/collections/collection_2018/eccc/En57-23-1-79-eng.pdf (accessed 2024 October 22)

McGregor G. 2024. Heatwaves: Causes, consequences and responses. Springer International Publishing, Durham. https://doi.org/10.1007/978-3-031-69906-1

Michelozzi P, Accetta G, De Sario M, D'Ippoliti D, Marino C, Baccini M, Biggeri A, Anderson HR, Katsouyanni K, Ballester F, Bisanti L, Cadum E, Forsberg B, Forastiere F, Goodman PG, Hojs A, Kirchmayer U, Medina S, Paldy A, Schindler C, Sunyer J, Perucci CA. 2009. High temperature and hospitalizations for cardiovascular and respiratory causes in 12 European cities. American Journal of Respiratory and Critical Care Medicine 179: 383-389. https://doi.org/10.1164/rccm.200802-217OC

Miller R, Golab L, Rosenberg C. 2017. Modelling weather effects for impact analysis of residential time-of-use electricity pricing. Energy Policy 105: 534-546. https://doi.org/10.1016/j.enpol.2017.03.015

Mohammad-Harmay NS, Choi M. 2022. Effects of heat waves on urban warming across different ur-

ban morphologies and climate zones. Building and Environment 209, 108677. https://doi.org/10.1016/j.buildenv.2021.108677

Morgan N, Gómez-Azpeitia G. 2018. Development of a Mexican standard of thermal comfort for naturally ventilated buildings. In: Rethinking comfort. Proceedings of 10th Windsor Conference (Brotas L, Roaf S, Nicol F, Humphreys M, Eds.). Windsor, UK, 596-607.

Narayanan A, Rezaali M, Bunting EL, Keellings D. 2025. It's getting hot in here: Spatial impact of humidity on heat wave severity in the U.S. Science of The Total Environment 963: 178397. https://doi.org/10.1016/j.scitotenv.2025.178397

Neethu C, Ramesh KV. 2022. Highresolution spatiotemporal variability of heatwave impacts quantified by thermal indices. Theoretical and Applied Climatology 148: 1181-1198. https://doi.org/10.1007/s00704-022-03987-9

Perkins SE, Alexander LV. 2013. On the measurement of heat waves. Journal of Climate 26: 4500-4517. https://doi.org/10.1175/JCLI-D-12-00383.1

Półrolniczak M, Tomczyk AM, Bednorz E. 2024. Biometeorological conditions in Poznań, Poland: Insights from in situ summer data. Atmosphere 15: 448. https://doi.org/10.3390/atmos15040448

Pyrgou A, Hadjinicolaou P, Satamouris M. 2020. Urban-rural moisture contrast: Regulator of the urban heat island and heatwaves' synergy over a Mediterranean city. Environmental Research 182: 109102. https://doi.org/10.1016/j.envres.2019.109102

Richard Y, Pohl B, Rega M, Pergaud J, Thevenin T, Emery J, Dudek J, Vairet T, Zito S, Chateau-Smith C. 2021. Is urban heat island intensity higher during hot spells and heat waves (Dijon, France, 2014-2019)? Urban Climate 35: 100747. https://doi.org/10.1016/j.uclim.2020.100747

Ripple WJ, Wolf C, Gregg JW, Rockström J, Mann ME, Oreskes N, Lenton TM, Rahmstorf S, Newsome TM, Xu Ch, Svenning JC, Pereira CC, Law BE, Crowther TW. 2024. The 2024 state of the climate report: Perilous times on planet Earth. BioScience 74: 812-824. https://doi.org/10.1093/biosci/biae087

Robine JM, Cheung SLK, Le Roy S, Van Oyen H, Griffiths C, Michel JP, Herrmann FR. 2008. Death toll exceeded 70,000 in Europe during the summer of 2003. Comptes Rendus Biologies 331: 171-178 (Dossier: Nouveautés en cancérogenèse). https://doi.org/10.1016/j.crvi.2007.12.001

Roshan GhR, Farrokhzad M, Attia S. 2017. Defining thermal comfort boundaries for heating and cooling demand estimation in Iran's urban settlements. Building and Environment 121: 168-189. https://doi.org/10.1016/j.buildenv.2017.05.023

Salau RA, Adelodun B, Ahmad MJ, Adeyi Q, Akinsoji AH, Odey G, Choi KS. 2025. Impact assessment of land-use and land-cover on urban heat wave using remote sensing and machine learning algorithms. International Journal of Environmental Science and Technology 22: 14369-14382. https://doi.org/10.1007/s13762-025-06569-0

SMN. 2024. Normales climatológicas por estado. Valores extremos. Servicio Meteorológico Nacional, México. Available at: https://smn.conagua.gob.mx/tools/RESOURCES/Normales_Climatologicas/Med-Extr/pue/medex21065.txt (accessed 2024 October 15)

SPCGIR. 2018. Programa Municipal de Protección Civil del Municipio de Puebla 2018-2021. Secretaría de Protección Civil y Gestión Integral del Riesgo-Protección Civil de la República Mexicana-Colegio Mexicano de Profesionales en Gestión de Riesgos y Protección Civil. Available at: https://memorias.pueblacapital.gob.mx/images/PMPC_Version_Final.pdf (accessed 2024 December 8)

Stewart ID, Oke TR. 2012. Local climate zones for urban temperature studies. Bulletin of the American Meteorological Society 93: 1879-1900. https://doi.org/10.1175/BAMS-D-11-00019.1

Stewart RE, Betancourt D, Davies JB, Harford D, Klein Y, Lannigan R, Mortsch L, O'Connell E, Tang K, Whitfield PH. 2017. A multi-perspective examination of heat waves affecting Metro Vancouver: Now into the future. Natural Hazards 87: 791-815. https://doi.org/10.1007/s11069-017-2793-7

Sung TI, Wu PC, Lung SC, Lin CY, Chen MJ, Su HJ. 2013. Relationship between heat index and mortality of 6 major cities in Taiwan. Science of The Total Environment 442: 275-281. https://doi.org/10.1016/j.scitotenv.2012.09.068

Tejeda-Martínez A, Balderas-Romero G, Moreyra-González LE, Castro-Díaz JO. 2023. Urban atmospheric humidity excesses and deficits in two Mexican metropolises: Guadalajara and Puebla. Atmósfera 38: 187-216. https://doi.org/10.20937/ATM.53252

Vargas N, Magaña V. 2020. Climatic risk in the Mexico City metropolitan area due to urbanization. Urban Climate 33: 100644. https://doi.org/10.1016/j.uclim.2020.100644

Vidal-Zepeda R, Hernández-Cerda ME. 2007. Naturaleza y ambiente. Climas (NA IV): Texto explicativo. In: Nuevo atlas de México (NA IV 3-4) (Coll-Hurtado A, Ed.). Instituto de Geografía, Universidad Nacional Autónoma de México.

Voosen P. 2024. El Niño fingered as likely culprit in record 2023 temperatures. Science 386: 137. https://doi.org/10.1126/science.adt7207

Wang P, Zhang W, Liu J, He P, Wang J, Huang L, Zhang B. 2023. Analysis and intervention of heatwave related economic loss: Comprehensive insights from supply, demand, and public expenditure into the relationship between the influencing factors. Journal of Environmental Management 326: 116654. https://doi.org/10.1016/j.jenvman.2022.116654

WMO. 2024. State of the climate in Latin America and the Caribbean 2023. WMO-No. 1351. World Meteorological Organization, Geneva. Available at: https://library.wmo.int/records/item/68891-state-of-the-climate-in-latin-america-and-the-caribbean-2023 (accessed 2024 October 22)

Yildiz B, Bilbao JI, Sproul AB. 2017. A review and analysis of regression and machine learning models on commercial building electricity load forecasting. Renewable and Sustainable Energy Reviews 73: 1104-1122. https://doi.org/10.1016/j.rser.2017.02.023

Zhang X, Alexander L, Hegerl GC, Jones P, Tank AK, Peterson TC, Trewin B, Zwiers FW. 2011. Indices for monitoring changes in extremes based on daily temperature and precipitation data. WIREs Climate Change 2: 851-870. https://doi.org/10.1002/wcc.147

Zhou W, Wang Q, Li R, Zhang Z, Kadier A, Wang W, Zhou F, Ling L. 2024. Heatwave exposure in relation to decreased sleep duration in older adults. Environment International 183: 108348. https://doi.org/10.1016/j.envint.2023.108348

Zhou X, Li Y, Xiao C, Chen W, Mei M, Wang G. 2025. High-impact extreme weather and climate event in China: Summer 2024 overview. Advances in Atmospheric Sciences 42: 1064-1076. https://doi.org/10.1007/s00376-024-4462-6

Zou Z, Yan C, Yu L, Jiang X, Ding J, Qin L, Wang B, Qiu G. 2021. Impacts of land use/land cover types on interactions between urban heat island effects and heat waves. Building and Environment 204: 108138. https://doi.org/10.1016/j.buildenv.2021.108138